

Coupling effects of chemical stresses and external mechanical stresses on diffusion

To cite this article: Fu-Zhen Xuan *et al* 2009 *J. Phys. D: Appl. Phys.* **42** 015401

View the [article online](#) for updates and enhancements.

Related content

- [Stress in film/substrate system due to diffusion and thermal misfit effects](#)
Shan-Shan Shao, Fu-Zhen Xuan, Zhengdong Wang *et al.*
- [Shear-lag model of diffusion-induced buckling of core-shell nanowires](#)
Yong Li, Kai Zhang, Bailin Zheng *et al.*
- [Effect of grain boundary trapping kinetics on diffusion in polycrystalline materials: hydrogen transport in Ni](#)
Dmitrii N Ilin, Anton A Kutsenko, Dome Tanguy *et al.*

Recent citations

- [Coupled chemomechanical theory with strain gradient and surface effects](#)
Wenyuan Liu and Shengping Shen
- [Fully Coupling Chemomechanical Yield Theory Based on Evolution Equations](#)
Wenyuan Liu *et al*
- [Analysis of oxygen exchange-limited transport and chemical stresses in perovskite-type hollow fibers](#)
Alexander Zolochovsky *et al*



LIVE WEBINAR

NanoRaman: Correlated Tip-Enhanced Optical Spectroscopy and Scanning Probe Microscopy

Thursday 8 March 15.00 GMT

REGISTER NOW!

physicsworld.com

Coupling effects of chemical stresses and external mechanical stresses on diffusion

Fu-Zhen Xuan¹, Shan-Shan Shao, Zhengdong Wang and Shan-Tung Tu

Key Laboratory of Safety Science of Pressurized System, MOE School of Mechanical Engineering, East China University of Science and Technology, 130, Meilong Street, PO Box 402 Shanghai 200237, People's Republic of China

E-mail: fzxuan@ecust.edu.cn

Received 29 July 2008, in final form 9 October 2008

Published 4 December 2008

Online at stacks.iop.org/JPhysD/42/015401

Abstract

Interaction between diffusion and stress fields has been investigated extensively in the past. However, most of the previous investigations were focused on the effect of chemical stress on diffusion due to the unbalanced mass transport. In this work, the coupling effects of external mechanical stress and chemical stress on diffusion are studied. A self-consistent diffusion equation including the chemical stress and external mechanical stress gradient is developed under the framework of the thermodynamic theory and Fick's law. For a thin plate subjected to unidirectional tensile stress fields, the external stress coupled diffusion equation is solved numerically with the help of the finite difference method for one-side and both-side charging processes. Results show that, for such two types of charging processes, the external stress gradient will accelerate the diffusion process and thus increase the value of concentration while reducing the magnitude of chemical stress when the direction of diffusion is identical to that of the stress gradient ($\vec{M} \cdot \vec{D} = 1$). In contrast, when the direction of diffusion is opposite to that of the stress gradient ($\vec{M} \cdot \vec{D} = -1$), the external stress gradient will obstruct the process of solute penetration by decreasing the value of concentration and increasing the magnitude of chemical stress. For both-side charging process, compared with that without the coupling effect of external stress, an asymmetric distribution of concentration is produced due to the asymmetric mechanical stress field feedback to diffusion.

1. Introduction

Diffusion of atoms is a very common phenomenon in many fields such as oxidation, absorption and desorption, metal creep and materials joining and bonding. This process in solid solution is known to cause the evolution of local stresses due to unbalanced mass transport, which has been referred to as diffusion-induced stresses or chemical stresses.

The evolution of chemical stresses in a thin plate during diffusion was originally analysed and an expression for residual stress in silicon wafer was developed by Prussin [1]. Then Li [2] studied the chemical stresses in the elastic media of simple geometries. Larche and Cahn [3, 4] investigated the stress dependence of the local diffusion flux in a solid where the stresses developed from composition inhomogeneities. Lee *et al* [5, 6] made a series of studies of chemical stresses

in specimens of different geometries such as thin plates, solid cylinders, hollow cylinders and solid spheres. Zhang *et al* [7] studied the effects of absorption and desorption on the chemical stress field in a membrane during permeation or both-side charging of a diffusing specimen, wherein the flux continuity (FC) boundary conditions were adopted. Recently, Ko *et al* [8] investigated the chemical stresses in a square sandwich composite with two different diffusion processes by the numerical method.

Another challenging issue in studying diffusion is the effect of diffusion-induced stresses on the material/component performance. For example, it has been realized that chemical stresses could affect the performance and reliability of microelectromechanical systems (MEMS), sensors and actuators [9, 10]. According to Kodentsov *et al*'s report [11], a periodic layer was formed in various ternary and higher order material systems due to metal/metal and metal/ceramic diffusion. Daruka *et al* [12] found that the curvature of

¹ Author to whom any correspondence should be addressed.

samples, caused by the chemical stresses, is proportional to the annealing time and the difference in the intrinsic diffusion coefficients. In addition, the chemical stress induced by the composition inhomogeneity in microelectronic devices could initiate the dislocation and affect the distribution of impurities and the behaviour of electronic devices [13]. Moreover, studies have shown that diffusion of hydrogen into metals could cause hydrogen-induced cracking and hydrogen-enhanced local plasticity and thus endanger the safety of nuclear plants [14].

Recently, considerable attention was paid to the interaction between chemical stresses and diffusion. Larche and Cahn [3] were pioneers in the research on the coupling between diffusion and chemical stresses. Then Chu and Lee [15] conducted an analysis for the effects of chemical stresses on diffusion. They found that the chemical stresses enhance the mass transfer and the effective diffusivity arising from the chemical stresses is proportional to the concentration. Zhang *et al* [16] re-analysed the distribution of the steady-state concentration of hydrogen in elastic membranes during hydrogen diffusion. However, it should be pointed out that Chu and Lee [15] and Zhang *et al*'s [16] research works were both implemented on the basis of Li's solution [2], but the coupling effect of chemical stress and diffusion was not included in Zhang *et al*'s work. Furthermore, Aziz [17] analysed the effects of pressure and stress on diffusion from the atomic point of view. Hwang *et al* [18] investigated the interaction of the self-induced electric field and the diffusion-induced stresses in a long bar with square cross section. Wang *et al* [19] investigated the effect of chemical stress on diffusion in a hollow cylinder for plane strain and zero axial force and found that chemical stresses could enhance both the diffusion coefficient and the concentration. Yang [20] developed a new relation between the hydrostatic stress and the concentration of solute atoms and pointed out that the linear distribution of solute atoms in the thin plate was non-existent due to the interaction between chemical stresses and diffusion.

However, it is worth noting that the existing studies were focused on chemical stresses and their effects on material behaviour and diffusion process. Actually, components or samples with diffusion of atoms are ineluctably subjected to external loadings or stress gradient. In many cases, the influence of external stresses on the diffusion process, especially the coupling effect with chemical stresses, is so significant that it cannot be neglected [21]. This prompts us to investigate the coupling effects of chemical stress and external mechanical stresses on the diffusion process.

The purpose of this investigation is to examine how the external stress and chemical stress induced in diffusion affect the process of solute penetration. For a thin plate subjected to a unidirectional tensile stress field, the finite difference method is employed to solve the external stress coupled diffusion equation for both one-side and both-side charging processes with the FC boundary conditions. This paper consists of the following sections.

- (1) Diffusion model development for the coupling issue of external mechanical stress and chemical stress.

- (2) One-side charging and both-side charging analysis for a thin plate subjected to the unidirectional tensile stress field.
- (3) Chemical stress evolution in consideration of the external mechanical stress effect.
- (4) Development of the concentration under the coupling effect of external mechanical stress and diffusion-induced (chemical) stress.

2. Diffusion model of the coupling problem

For the present purpose, we only focus on the small deformation and assume the material to be an isotropic elastic solid. In terms of thermodynamic theory, the chemical potential, μ , in an ideal solid solution subjected to external stresses can be written as [2]

$$\mu = \mu_0 + RT \ln C - \sigma_h \bar{V}, \quad (1)$$

where μ_0 is a constant; R , T and \bar{V} are the gas constant, the temperature in Kelvin and the partial molar volume of solute ($\text{cm}^3 \text{atom}^{-1}$), respectively. C and σ_h are the concentration (atoms cm^{-3}) of the diffusing component and the hydrostatic stress, respectively. \bar{V} is assumed to be independent of time and concentration C .

In addition, the characteristic time for elastic deformation of solids is very small compared with that of atomic migration in solids. Therefore, the elastic deformation can be treated as a quasi-static state [20]. As a consequence, the formal theory of linear elasticity is applicable for the coupling case of chemical stresses and external stresses. The hydrostatic stress in the solid subjected to the combined stresses due to the concentration gradient and the external loading can be expressed as

$$\sigma_h = \frac{1}{3} \sum_{i=x,y,z} (\sigma_{ci} + \sigma_{ei}), \quad (2)$$

where σ_{ci} denotes the chemical normal stress and σ_{ei} is the external normal mechanical stress, respectively.

The gradient of chemical potential is the driving force of mass transport and is proportional to the diffusion flux [2], i.e. $\vec{J} = -NC\vec{\nabla}\mu$, where \vec{J} is the vector of the diffusion flux and N is the solute mobility and is independent of time. In terms of equation (1), the diffusion flux can be expressed as

$$\vec{J} = -D_{\text{eff}} \vec{\nabla} C = -NRT \left(1 + C \frac{\partial \sigma_h}{\partial C} \right) \vec{\nabla} C, \quad (3)$$

where D_{eff} is the effective diffusivity of solute in a stressed isotropic solid. Referring to equation (2), D_{eff} can be calculated by

$$D_{\text{eff}} = D_0 \left(1 - \frac{\bar{V}C}{RT} \frac{\partial \sigma_h}{\partial C} \right) = D_0 \left\{ 1 - \frac{\bar{V}C}{3RT} \frac{\partial \left[\sum_{i=x,y,z} (\sigma_{ci} + \sigma_{ei}) \right]}{\partial C} \right\}, \quad (4)$$

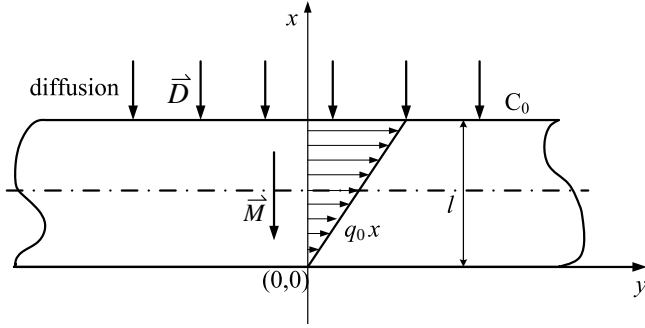


Figure 1. Schematics of a thin plate subjected to an applied unidirectional tensile stress field.

where D_0 is the diffusivity of solute in a stress-free isotropic solid and is defined by

$$D_0 = NRT. \quad (5)$$

Apparently, D_{eff} is concentration dependent and is a function of time since the concentration varies with time.

Using the law of mass conservation,

$$\vec{\nabla} \cdot \vec{J} = -\frac{\partial C}{\partial t}. \quad (6)$$

Substituting equation (3) into equation (6), the diffusion equation including the coupling effect of chemical stresses and external mechanical loadings is obtained by

$$D_0 \left\{ \nabla^2 C - \frac{\bar{V}}{3RT} \vec{\nabla} C \cdot \vec{\nabla} \left[\sum_{i=x,y,z} (\sigma_{ci} + \sigma_{ei}) \right] - \frac{\bar{V}C}{3RT} \nabla^2 \left[\sum_{i=x,y,z} (\sigma_{ci} + \sigma_{ei}) \right] \right\} = \frac{\partial C}{\partial t}. \quad (7)$$

3. Diffusion in an external bent thin plate

3.1. Model description

Consider a thin plate of isotropic material subjected to a unidirectional gradient stress field, as shown in figure 1. \vec{M} denotes the direction of stress gradient induced by external mechanical loading. \vec{D} is the direction of diffusion. Therefore, two different cases should be considered, $\vec{M} \cdot \vec{D} = 1$ and $\vec{M} \cdot \vec{D} = -1$.

Analogous to thermal stresses [1], for a given concentration distribution C , two equal transverse stresses are produced in the plate and could be approximately expressed as

$$\sigma_{cy} = \sigma_{cz} = \frac{E}{1-\nu} \frac{\bar{V}}{3} \left(\bar{C} - C + \frac{6(2x-l)}{l^3} \times \int_0^l \left(x - \frac{l}{2} \right) C dx \right), \quad (8)$$

where l , E and ν are the thickness of the plate, Young's modulus and Poisson's ratio, respectively. \bar{C} is the average concentration through the thickness of the plate, $\bar{C} = 1/l \int_0^l C dx$. Generally, the elastic constants E , ν and the partial molal volume may vary slightly due to mass transport.

However, in this work, we assume that E , ν and \bar{V} are unchanged with the concentration for simplicity.

Generally, the thin plate may be subjected to a unidirectional gradient stress field due to the loading combination of tensile and mechanical bending. As depicted in figure 1, the unidirectional gradient stress field can be expressed by

$$\sigma_{ey} = f_0 + q_0 x, \quad \sigma_{ex} = \sigma_{ez} = 0, \quad (9)$$

where f_0 denotes the tensile stress and q_0 is the stress gradient due to mechanical bending and is a constant for linear distribution.

Substituting the chemical stress equation (8) and external stress equation (9) in equation (7) yields

$$\frac{\partial C}{\partial t} = D_0 \left\{ (1 + FC) \frac{\partial^2 C}{\partial x^2} + F \left(\frac{\partial C}{\partial x} \right)^2 - \frac{12F}{l^3} \frac{\partial C}{\partial x} \int_0^l \left(x - \frac{l}{2} \right) C dx - \frac{\bar{V}}{3RT} \frac{\partial C}{\partial x} q_0 \right\}, \quad (10)$$

where

$$F = \frac{2E\bar{V}^2}{9(1-\nu)RT}. \quad (11)$$

Therefore, the above-defined effective diffusivity of solute in a stressed isotropic solid D_{eff} becomes

$$D_{\text{eff}} = D_0 \left(1 + FC - \frac{12FC}{l^3 (\partial C / \partial x)} \int_0^l \left(x - \frac{l}{2} \right) C dx - \frac{\bar{V}Cq_0}{3RT (\partial C / \partial x)} \right). \quad (12)$$

3.2. Boundary conditions

In general, we take the electrochemical permeation process as an example which involves the surface effects as studied by Zhang and Zheng [22]. For the permeation tests, there are four different boundary conditions developed to evaluate the hydrogen diffusivity, i.e. constant concentration (CC), constant flux (CF), FC, and hybrid of flux continuity and constant concentration (FCCC). Comparisons between the predictions from the above different boundary conditions and experimental results have been conducted by Zhang *et al* [23]. They pointed out that the CF model could lead to three times higher hydrogen diffusivity than that from the CC model, and the dependence of the sample thickness and surface conditions was also observed. Although the FCCC model could well explain the permeation flux at steady state, various desorption rates and absorption parameters were extracted from the FCCC model for different samples. However, the FC model could lead to a thickness-independent desorption rate and absorption parameter at a given charging current density and hence was suggested as the best one to describe the electrochemical permeation test. In this paper, the FC boundary condition is therefore employed in the analysis of one-side charging and both-side charging processes.

For the one-side charging process, the thickness of the plate is taken as l . The entry side and the exit side surfaces

are located at $x = 0$ and $x = l$, respectively. For the both-side charging process, the thickness is taken as $2l$. Initially, no solute atom is in the solid, i.e.

$$C = 0 \quad \text{at } t = 0, \quad (13)$$

and the boundary conditions are

$$\begin{cases} \frac{\partial C}{\partial x} = 0 & \text{at } x = 0 \\ D_{\text{eff}} \frac{\partial C}{\partial x} + kC = k_p & \text{at } x = l \end{cases} \quad \text{for } t > 0 \quad (14)$$

for one-side charging and

$$\begin{cases} D_{\text{eff}} \frac{\partial C}{\partial x} + kC = k_p & \text{at } x = l \\ D_{\text{eff}} \frac{\partial C}{\partial x} - kC = -k_p & \text{at } x = -l \end{cases} \quad \text{for } t > 0 \quad (15)$$

for both-side charging. Here k is the desorption rate constant and k_p is the forward flux of the permeating atoms or molecules from the outside into the sample at the entry surface.

3.3. Finite difference method

Referring to Zhang and Zheng's work [22], the drift velocity on the surface $V_s = k$, the drift velocity in bulk $V_b = D_0/l$ and the permeation concentration $C_0 = k_p/k$ were introduced. Furthermore, the following dimensionless parameters for length x' , concentration C' , time t' , external mechanical stress gradient M' and dimensionless parameter F' were also introduced:

$$x' = x/l, \quad (16a)$$

$$C' = C/C_0, \quad (16b)$$

$$t' = D_0 t/l^2, \quad (16c)$$

$$F' = F C_0, \quad (16d)$$

$$M' = \frac{\bar{V}}{3RT} q_0 l. \quad (16e)$$

For the one-side charging process, diffusion equation (10) and boundary condition (14) were thus normalized to

$$\begin{aligned} \frac{\partial C'}{\partial t'} &= (1 + F' C') \frac{\partial^2 C'}{\partial x'^2} + F' \left(\frac{\partial C'}{\partial x'} \right)^2 \\ &\quad - 12 F' \frac{\partial C'}{\partial x'} \int_0^1 \left(x' - \frac{1}{2} \right) C' dx' - M' \frac{\partial C'}{\partial x'}, \end{aligned} \quad (17)$$

$$\begin{cases} \frac{\partial C'}{\partial x'} = 0 & \text{at } x' = 0 \\ (1 + F' C') \frac{\partial C'}{\partial x'} - 12 F' C' \int_0^1 \left(x' - \frac{1}{2} \right) C' dx' \\ - M' C' + \frac{V_s}{V_b} C' = \frac{V_s}{V_b} & \text{at } x' = 1. \end{cases} \quad (18)$$

Apparently, the concentration is an even function of x for the both-side charging process and the third term of equation (10) on the right side is zero due to the geometric

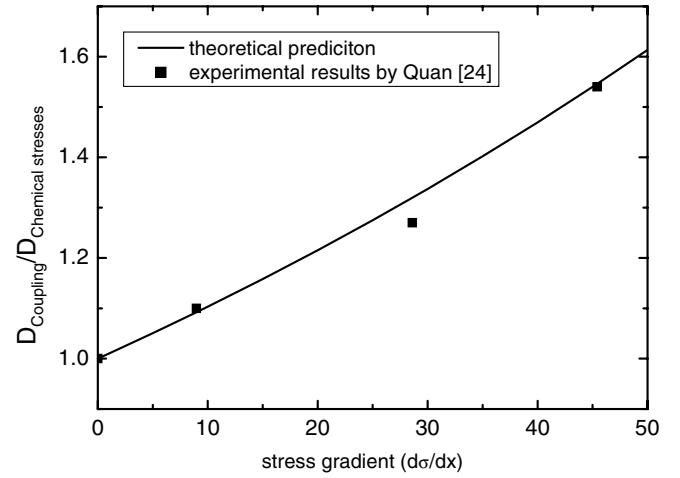


Figure 2. Comparisons of normalized diffusivities from the experimental results and theoretical predictions with various values of external stress gradient ($\bar{M} \cdot D = 1$, $D_0 t/l^2 = 3 \times 10^{-5}$).

symmetry. Therefore, the diffusion equation under external stress becomes

$$\frac{\partial C}{\partial t} = D_0 \left\{ \frac{\partial^2 C}{\partial x^2} + F \left[C \frac{\partial^2 C}{\partial x^2} + \left(\frac{\partial C}{\partial x} \right)^2 \right] - \frac{\bar{V} q_0}{3RT} \frac{\partial C}{\partial x} \right\}. \quad (19)$$

Then equation (19) and boundary condition (15) can be normalized to

$$\frac{\partial C'}{\partial t'} = (1 + F' C') \frac{\partial^2 C'}{\partial x'^2} + F' \left(\frac{\partial C'}{\partial x'} \right)^2 - M' \frac{\partial C'}{\partial x'}. \quad (20)$$

$$\begin{cases} (1 + F' C') \frac{\partial C'}{\partial x'} - M' C' + \frac{V_s}{V_b} C' = \frac{V_s}{V_b} & \text{at } x' = 1 \\ (1 + F' C') \frac{\partial C'}{\partial x'} - M' C' - \frac{V_s}{V_b} C' = -\frac{V_s}{V_b} & \text{at } x' = -1. \end{cases} \quad (21)$$

Equation (17) with (18) and equation (20) with (21) are numerically solved by using the finite difference method. The space derivative and time derivative are calculated by the central difference and forward difference, respectively. The integral is calculated using Simpson's rule. The dimensionless thickness of the plate is divided into 200 equal parts, i.e. $\Delta x' = 0.005$. The dimensionless time increment is set to be $\Delta t' = 0.001$.

To verify the above proposed model, the results of hydrogen penetration tests under unidirectional tensile stress fields by Quan [24] are referred to herein. For the hydrogen diffusion direction (\vec{D}) being identical to the direction of the external stress gradient (\vec{M}), the normalized diffusivity, $D_{\text{Coupling}}/D_{\text{Chemical stresses}}$, from the prediction of the proposed model and experimental results is shown in figure 2 at $D_0 t/l^2 = 3 \times 10^{-5}$ with various normalized external stress gradients M' . As expected, good agreement is observed between the prediction and the experimental results. This gives us confidence in the application of the proposed model for the coupling effect analysis.

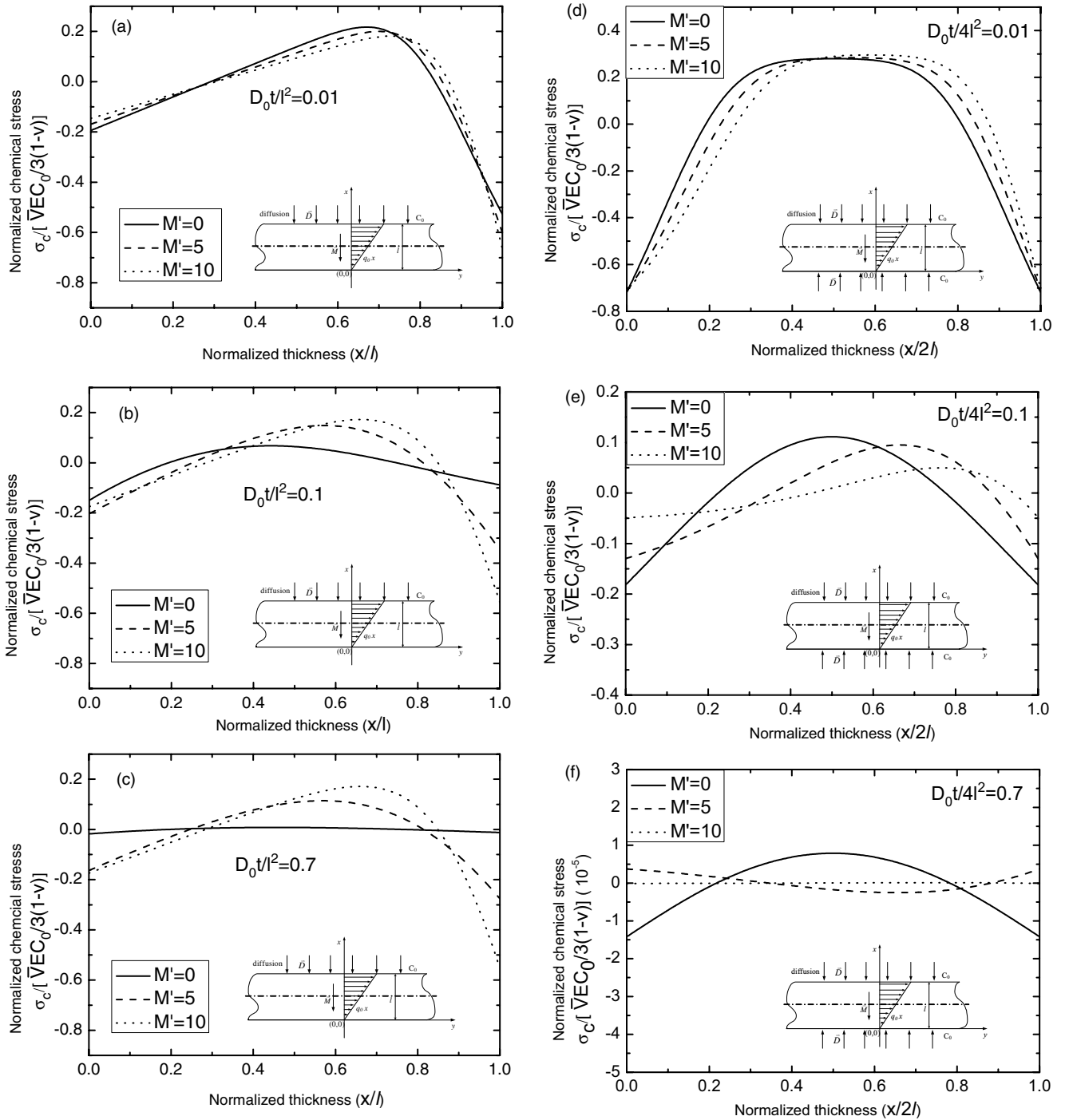


Figure 3. The chemical stress profiles for different external stress gradients with various times during the permeation process. (a)–(c) For one-side charging; (d)–(f) for both-side charging (where $V_s/V_b = 100$ and $FC_0 = 0.5$).

4. Results and discussion

4.1. Evolution of chemical stress

The profiles of chemical stresses in the thin plate subjected to different external stress gradients at different times for one-side charging and both-side charging processes are shown in figure 3, where $V_s/V_b = 100$, $FC_0 = 0.5$. From figure 3, it can be seen that, for the two types of charging processes discussed herein, the chemical stresses are compressive in the

regions near the entry and exit surfaces while opposite in the direction in the central region. In addition, the maximum of chemical stress is always located at the entry surface at a given time. When the external stress gradient is small, no significant change is observed. Another interesting observation is that, with the diffusion time increasing, the external stress gradient displays a significant influence on the evolution of chemical stresses. Such an influence will increase with increasing external stress gradient.

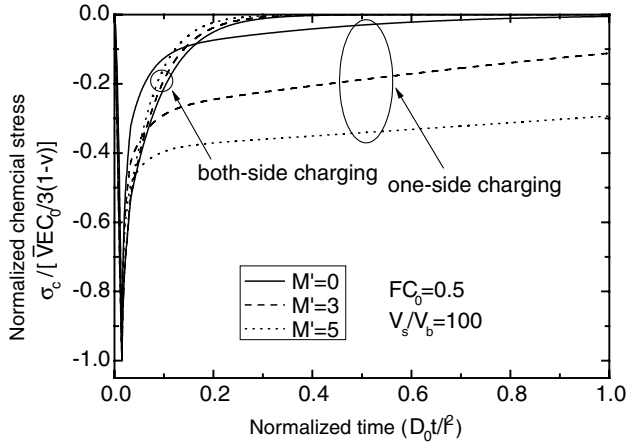


Figure 4. Chemical stresses at the entry surface for various values of external stress gradients (where $V_s/V_b = 100$ and $FC_0 = 0.5$).

However, it is also worth noting that, for one-side and both-side charging processes, different influence trends are observed for chemical stress due to the interaction of external stress and diffusion. For the one-side charging process, the external stress will increase the chemical stress compared with that with lower external stress gradient or without external stress at a given time, as shown in figures 3(a)–(c). For the both-side charging process, asymmetric distribution of chemical stresses occurs through the thickness of plate due to the coupling effect of asymmetrically distributed external stress, as shown in figures 3(d)–(f), in contrast to the result of effects of absorption and desorption on the chemical stress field given by Zhang *et al* [7]. The curves are concave for a short time and gradually become straight when steady state is reached. On the other hand, larger external stresses are inclined to decrease the value of chemical stress compared with that with lower external stress gradient as time increases, as shown in figures 3(e)–(f).

Figure 4 shows the evolution of chemical stresses at the entry surface versus time for various external stress gradients M' , where $V_s/V_b = 100$, $FC_0 = 0.5$. As expected, for both types of permeation processes, the magnitude of chemical stress at the entry surface increases with increasing time to a maximum and then decreases gradually as the charging process goes on. However, no significant difference in the maximum magnitudes of chemical stresses is observed for different external stress gradients. For the case of the diffusion direction being opposite to that of the external stress gradient ($\vec{M} \cdot \vec{D} = -1$), the magnitude of chemical stress increases with increasing external stress and increasing diffusion time. It implies that for this case the charging at the entry surface will be slower when the external stress gradient becomes larger. The external stress gradient will impede the diffusion of solute atoms for this case. In consequence, the value of the concentration reduces and thus leads to the decrease in chemical stress coupling.

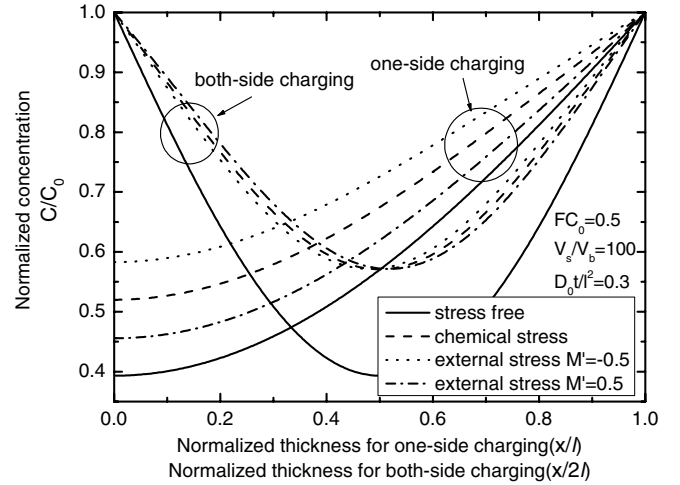


Figure 5. Concentration profiles for one-side and both-side charging processes with and without stress feedback to diffusion (where $V_s/V_b = 100$, $FC_0 = 0.5$ and $D_0 t / l^2 = 0.3$).

4.2. Development of concentration

Considering the coupling effect of external stress and chemical stress on the distribution of concentration, the following four different cases are discussed in this section: (a) different charging processes under the same external stress gradient; (b) different partial molal volumes of the mobile solute (FC_0); (c) various ratios of the drift velocity and (d) different external stress gradients.

At a given time $D_0 t / l^2 = 0.3$, the concentration profiles through the thickness of the thin plate are shown in figure 5 for one-side charging and both-side charging processes, where $V_s/V_b = 100$, $FC_0 = 0.5$. As expected, the distribution of the concentration is significantly affected by the external stress and chemical stress in comparison with that neglecting the stress feedback to diffusion. From figure 5, it is obvious that both external stress and chemical stresses will increase the value of concentration. According to the results of Ko *et al* [29], if the effects of chemical stresses are neglected, the concentration profile in one-side charging will be identical to the half concentration profile in both-side charging. When the external stress gradient exists discussed herein, the concentration profile in both types of charging processes will be different. At the same location where the normalized thickness is larger than 0.5, the concentration for one-side charging is greater than the concentration for both-side charging.

Among the four cases plotted in figure 5, the lowest value of concentration is observed where the stress effects have been neglected. The magnitude of concentration due to the effect of chemical stress alone is always located between those with two opposite directions of the external stress gradient. For both types of charging processes, when the direction of diffusion is identical to that of the stress gradient ($\vec{M} \cdot \vec{D} = 1$), the external stress gradient will promote the value of concentration and thus accelerate the solute penetration. This implies that external stress can be used to modify diffusion barriers because they can help to stabilize/destabilize strains originating inside the material and to accommodate the absorbed impurity [25–28]. According to Yet's experimental results [27], an enlarged

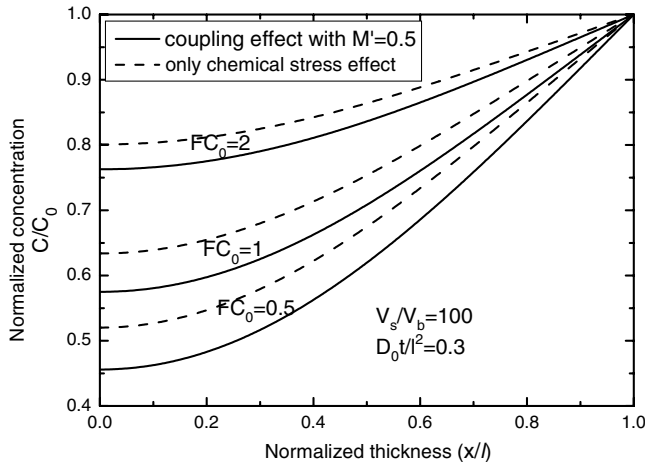


Figure 6. Concentration profiles for various values of FC_0 for one-side charging process with and without external stress effect (where $V_s/V_b = 100$ and $D_0t/l^2 = 0.3$).

atom spacing of silicon due to tensile mechanical stress will enhance the oxidation rate. Moreover, Sanchez's study [28] has shown that a tensile stress of 2 GPa increased or decreased the diffusion barrier by about 9% and altered the thermal diffusion by about 30% at room temperature.

In contrast, when the direction of diffusion is opposite to that of the stress gradient ($\vec{M} \cdot \vec{D} = -1$), the external stress gradient will decrease the value of concentration and thus obstruct the process of solute penetration. For the both-side charging process, furthermore, compared with that without the coupling effect of external stress, it is interesting to note that asymmetric distribution of the concentration is produced due to the mechanical stress feedback to diffusion. This finding agrees very well with the results obtained by Quan [24] through the electrochemical permeation test in an applied stress field.

Figure 6 shows the coupling effects of external and chemical stresses on the concentration distribution corresponding to various partial molal volumes of the mobile solute, which is proportional to FC_0 , for one-side charging where $V_s/V_b = 100$ and $D_0t/l^2 = 0.3$. Obviously, the concentrations increase with increasing FC_0 , both chemical stress alone and coupling effects of external stress and chemical stress. Again, a lower concentration is achieved when the diffusion direction is opposite to the direction of the external stress gradient ($\vec{M} \cdot \vec{D} = -1$) compared with that under chemical stress alone.

To illustrate the interaction of external stress with various values of V_s/V_b , the concentration distribution through the thickness of plate is computed and shown in figure 7. At a given time, it can be seen that the concentration at both the entry surface and the exit surface increases with increasing V_s/V_b whether the external stress is coupled or not. This is because a large V_s/V_b means that there is a low energy barrier for solute atoms to overcome [23]. However, the decrement in concentration due to the coupling effect of the external stress will increase with increasing values of V_s/V_b . The difference in concentration between that under the coupling of external stress and chemical stress and that under chemical stress alone will fade away when the value of V_s/V_b approaches unity, for

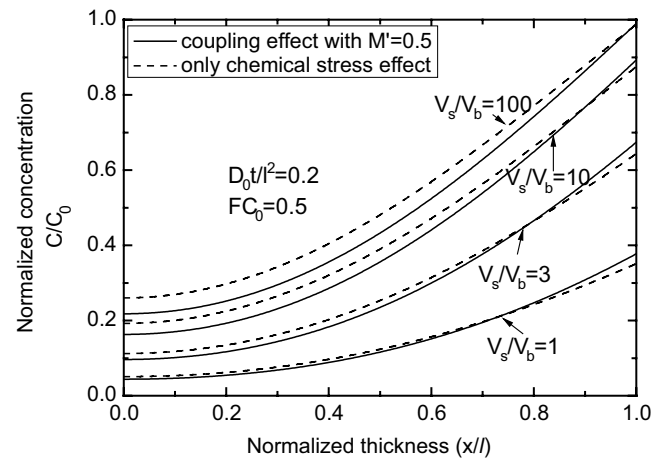


Figure 7. Concentration profiles for various ratios of the drift velocities for one-side charging process with and without the external stress effect ($FC_0 = 0.5$, $D_0t/l^2 = 0.2$).

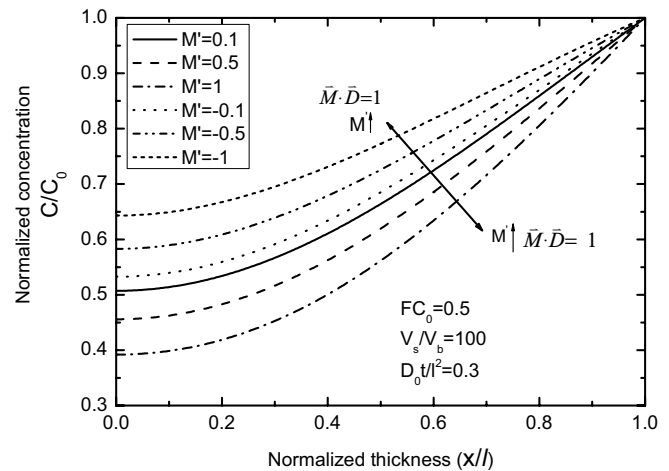


Figure 8. Concentration profiles for various values of external stress gradients for one-side charging ($FC_0 = 0.5$, $V_s/V_b = 100$, $D_0t/l^2 = 0.3$).

example, $V_s/V_b = 1$ and $D_0t/l^2 = 0.2$ as shown in figure 7. The reason is that the absorption and desorption processes have a slight effect on diffusion for small V_s/V_b , especially at the entry surface, compared with the effect of the external stress gradient. In other words, the lower the value of V_s/V_b , the less dominant the surface effect, as discussed by Zhang *et al* [29, 30].

Effects of the external stress gradient on concentration profiles for one-side charging process are depicted in figure 8, where $FC_0 = 0.5$, $V_s/V_b = 100$, $D_0t/l^2 = 0.3$. It is worth noting that, when the direction of diffusion is identical to that of the stress gradient ($\vec{M} \cdot \vec{D} = 1$), i.e. M' is negative, the concentration increases with increasing magnitude of M' . This is due to the higher stress gradient enhancing the diffusion of solute atoms for this case. When the direction of diffusion is opposite to that of the stress gradient ($\vec{M} \cdot \vec{D} = -1$), i.e. M' is positive, the concentration decreases with increasing magnitude of M' . This can be used to explain the phenomenon

in Quan's [24] experiment why the measured diffusivity decreases with increasing absolute value of the stress gradient when $\vec{M} \cdot \vec{D} = -1$.

5. Concluding remarks

The coupling effects of chemical stresses and external mechanical stresses on diffusion are analysed. A self-consistent diffusion equation including the chemical stress and the external mechanical stress gradient has been developed based on Zhang *et al*'s [7, 29] work by using thermodynamic theory and Fick's law. For a thin plate of isotropic material subjected to unidirectional tensile stress fields, the diffusion equation coupled to the chemical stress and external mechanical stress has been solved numerically with the help of the finite difference method for one-side and both-side charging processes.

It is shown that external mechanical stresses play an essential role in these two types of processes. For such two types of charging processes, when the direction of diffusion is identical to that of the stress gradient, i.e. $\vec{M} \cdot \vec{D} = 1$, the external stress gradient will accelerate the diffusion process and thus increase the value of concentration and reduce the magnitude of chemical stress. In contrast, when the direction of diffusion is opposite to that of the stress gradient, i.e. $\vec{M} \cdot \vec{D} = -1$, the external stress gradient will obstruct the process of solute penetration and hence decrease the value of concentration and increase the magnitude of chemical stress. For the both-sides charging process, compared with that without the coupling effect of external stress, an asymmetric distribution of concentration is produced due to the asymmetric mechanical stress field feedback to diffusion.

Acknowledgments

The authors are grateful for the support provided by the National Natural Science Foundations of China (10672058), the Program for New Century Excellent Talents in University (NCET-06-0414) and the Shanghai Leading Academic Discipline Project (B503).

References

- [1] Prussin S 1961 *J. Appl. Phys.* **32** 1876–81
- [2] Li J C M 1981 *Scr. Metall.* **15** 21–8
- [3] Larche F C and Cahn J W 1982 *Acta Metall.* **30** 1835–45
- [4] Larche F C and Cahn J W 1984 *J. Res. Natl Bur. Stand.* **89** 467–500
- [5] Lee S, Wang W L and Chen J R 2000 *Mater. Chem. Phys.* **64** 123–30
- [6] Lee S, Wang W L and Chen J R 2000 *Mater. Sci. Eng. A* **285** 186–94
- [7] Zhang T Y, Ko S-C and Lee S 2002 *J. Appl. Phys.* **91** 2002–8
- [8] Ko S-C, Lee S and Chou Y T 2005 *Mater. Sci. Eng. A* **409** 145–52
- [9] Yang F Q and Li J C M 2003 *J. Appl. Phys.* **93** 9304–9
- [10] Begley M R, Utz M and Komaragiri U 2005 *J. Mech. Phys. Solids* **53** 2119–40
- [11] Kodentsov A A, Rijnders M R and Loo F J J 1998 *Acta Mater.* **46** 6521–8
- [12] Daruka I, Szabo I A, Beke D L, Cserhati C and Kodentsov A 1996 *Acta Mater.* **44** 4981–93
- [13] Levy R A 1989 *Microelectronic Materials and Process* (Boston, MA: Kluwer Academic) chapter 12
- [14] Metzger D R, Sauve R and Byrne T P 2006 *ASME Pressure Vessels and Piping Division Conference* ed M P P Paidoussis (New York: ASME) p 93664
- [15] Chu J L and Lee S 1994 *J. Appl. Phys.* **75** 2823–9
- [16] Zhang W S, Zhang X W and Zhang Z L 2000 *J. Alloys Compounds* **302** 258–63
- [17] Aziz M J 1997 *Appl. Phys. Lett.* **70** 2810
- [18] Hwang C-C, Lin S, Chu H-S and Lee W-S 1999 *Int. J. Solids Struct.* **36** 269–84
- [19] Wang W L, Lee S and Chen J R 2002 *J. Appl. Phys.* **91** 9584–90
- [20] Yang F Q 2005 *Mater. Sci. Eng. A* **409** 153–9
- [21] Limarga A M and Wilkinson D S 2007 *Acta Mater.* **55** 189–201
- [22] Zhang T Y and Zheng Y P 1998 *Acta Mater.* **46** 5023–33
- [23] Zhang T Y, Zheng Y P and Wu Q Y 1999 *J. Electrochem. Soc.* **146** 1741–50
- [24] Quan G F 1997 *Corrosion* **53** 99–102
- [25] Antonelli A, Kaxiras E and Chadi D J 1998 *Phys. Rev. Lett.* **81** 2088
- [26] Zhang X and Wang C Y 2006 *J. Phys. D: Appl. Phys.* **39** 4311–5
- [27] Yen J Y and Hwu J G 2000 *Appl. Phys. Lett.* **76** 1834–5
- [28] Sanchez J, Fullea J, Andrade C and Andres P L 2008 *Phys. Rev. B* **78** 014113
- [29] Ko S-C, Zhang T Y and Lee S 2007 *J. Appl. Phys.* **101** 113521–6
- [30] Zhang T Y and Zheng Y P 1998 *Acta Mater.* **46** 5035–43